

Author(s): Richard W. Peterson (presenter), Connor D. Fredrick, and Keith R. Stein, Bethel University, St. Paul, MN 55112, Phone 651-638-6465, petric@bethel.edu

Title: Interferometric Faraday effect magnetic field measurements

Abstract: The Faraday effect has ongoing applications including optical isolators and measuring dynamic magnetic fields in lab or space-based plasmas. A direct interferometric study of the circular birefringence underlying the Faraday effect provides a powerful platform for creative work in the undergraduate optics laboratory and makes clear the underlying physics. This workshop introduces a heterodyne interferometer for determining phase shifts between left- and right-handed circular polarizations as they pass through a substance in the direction of the magnetic field. Phase shifts due to magnetic fields within a commercially available 1.3 cm long terbium gallium garnet (TGG) crystal (after 3 passes of the 633 nm laser beam) can be plotted as a function of time – corresponding to $\mathbf{B}(t)$ down to the mT range. In the case of an broader advanced lab project format involving several weeks of time, the experiment may also provide a venue for introducing the use of heterodyne interferometers in measuring rapidly changing optical path length changes on the nanometer scale.

Experimental Documentation for Workshop – see pdf of detail student report for background and experimental details. [Detailed student experimental report with data, equipment, and procedure (of Doebrmann, Houlton, Watkins, and Youngblood) follows.] Snapshots of optical setups and a line drawing are below:

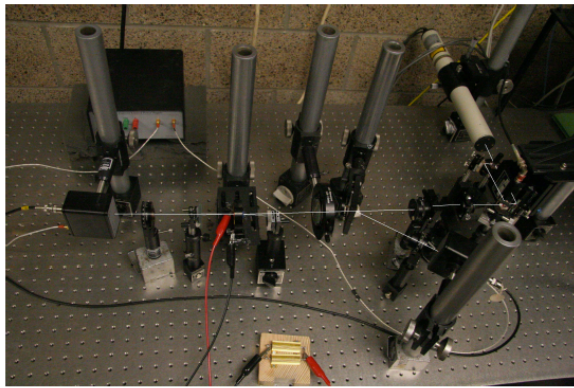


FIG. 8: The physical setup for our heterodyne interferometer with lines added to show the propagation of the light beams.

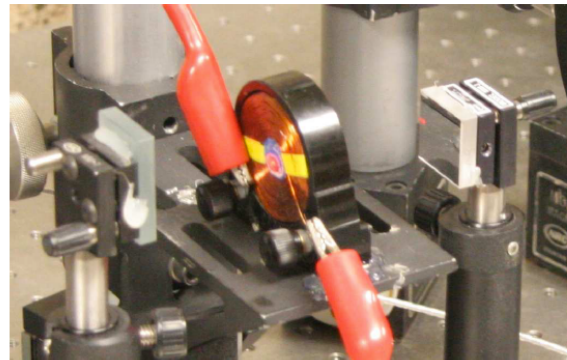


FIG. 9: Solenoid with TGG crystal at center. Mirrors are used to achieve five passes through the crystal causing a greater net rotation of the linear polarization.

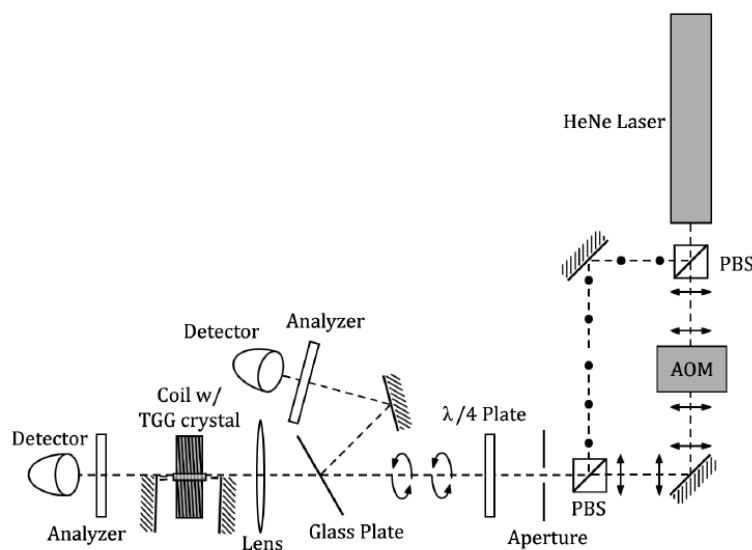


FIG. 7: Heterodyne Mach-Zehnder interferometer with TGG crystal. Magnetic fields parallel to the direction of propagation of light induce circular birefringence in the crystal, causing a net rotation in the linear polarization. This can be seen as a phase difference between the reference and signal beams.

Measurement of Faraday Rotation in Terbium Gallium Garnet with a Heterodyne Interferometer

Jessica Doehrmann, Jack Houlton, Justin Watkins, Nathan Youngblood
With Dr. Richard Peterson Advising
Bethel University Optics Lab

(Dated: May 14, 2010)

The Faraday Effect within a Terbium Gallium Garnet (TGG) crystal in conjunction with heterodyne interferometry can be used to make high precision measurements of magnetic fields in real time. This method is attractive for measuring magnetic fields due to its ability to measure a broad spectrum of field amplitudes and frequencies. Phase sensitive interferometric measurements were used to determine the magnitude of small amplitude and rapidly varying magnetic fields. The current instrument is capable of making real time magnetic field measurements resolved to 15 gauss. Period magnetic events were accurately measured with amplitudes as small as 2.42 ± 0.05 gauss. The high frequency capabilities of this system are limited only by high pass filtering and could be extended to the megahertz range. Additionally, Verdet's constant for 632.8 nm laser light in TGG was found to be temperature dependent with a value of $0.449 \pm 0.005 \frac{\text{min}}{\text{gauss*cm}}$ at the ambient lab temperature.

I. INTRODUCTION

A. The Faraday Effect

The Faraday Effect is a magneto-optical phenomenon which occurs in various materials. In this phenomenon, a magnetic field induces circular birefringence in a physical medium. If linearly polarized light is passed through such a birefringent medium, the light will experience a rotation of its linear polarization. This is because linearly polarized light can be thought of as the superposition of two orthogonal circular polarizations, one left rotating polarization and one right rotating polarization. From a classical standpoint, when circular, monochromatic light propagates through a material, elastically bound electrons within the material are set into circular orbits due to the rotating \vec{E} field. If an external magnetic field is applied perpendicular to the plane of orbit, the electrons will experience a magnetic force in the radial direction. This force may be either centrifugal or centripetal depending on the direction of the applied magnetic field and the direction of the circular polarization. This additional force is added to the elastic restoring force and results in two possible values for the total radial force and the radius of the electrons orbits. Thus, for a given magnetic field direction, two opposite circular polarizations will experience different electric dipole moments within the material and will therefore experience two different indices of refraction [1].

While propagating through a circularly birefringent medium, one circular polarization will experience a smaller index of refraction, allowing it to accumulate phase (relative to the opposite circular polarization), causing a net rotation of the linear polarization. The difference between the two indices of refraction for the two polarizations is directly proportional to the component of the magnetic field along the direction of propagation of light through any particular point in the material. For

a constant magnetic field, the angle of rotation of the linear polarization is directly proportional to both the magnetic field applied to the material and to the length of the material. The constant of proportionality relating these quantities is known as Verdet's constant. Verdet's constant is defined as the following:

$$V = \frac{\Delta\theta}{\int \vec{B} \cdot d\vec{l}} \quad (1)$$

Where \vec{B} is the magnetic field applied, $d\vec{l}$ is a vector differential length in the direction of the light's propagation vector, and $\Delta\theta$ is the angle of rotation of the linear polarization viewed in a plane which has a normal vector described by the light's propagation vector. This implies that if light is sent through a circularly birefringent material and reflected back again in the opposite direction, the rotation angle doubles rather than canceling.

For N passes through a material of length L , subjected to a constant magnetic field of magnitude B , aligned with the direction of propagation of the light through the material, equation 1 reduces to the following:

$$V = \frac{\Delta\theta}{NLB} \quad (2)$$

One material which strongly exhibits the Faraday Effect is Terbium Gallium Garnet (TGG), a crystalline dielectric with common uses in the field of optics. A TGG crystal was the birefringent material used in this research.

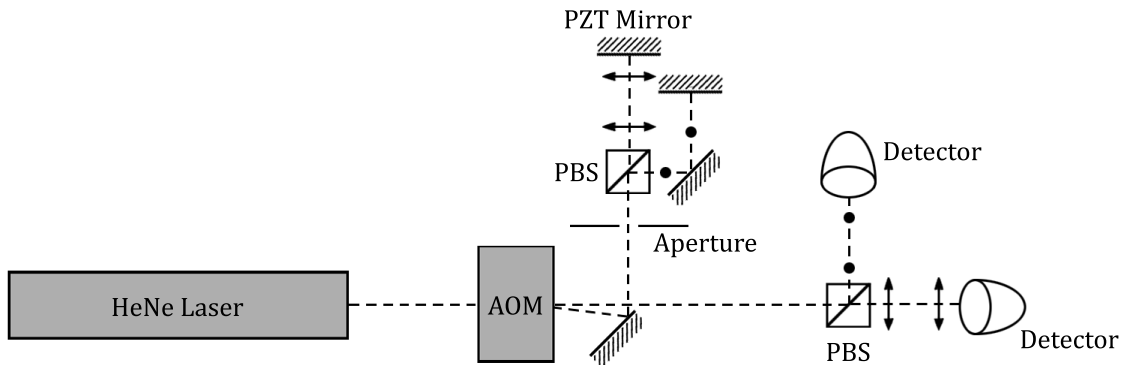


FIG. 1: A phase sensitive heterodyne Michelson interferometer. The reference and signal arms each have different polarizations that are both shifted from the laser frequency 80 MHz by two passes through an acousto-optic modulator. The signals from each arm are reflected off the output mirror of the laser, then interfere with the unshifted zero order beams at the detectors.

II. PROCEDURE

A. Interferometry

1. Heterodyne Michelson Interferometer

Interferometry is among the most widely applied methods for precision measurement in physics. By utilizing the coherent nature of laser light, one is able to make measurements on the order of nanometers. In order to gain experience with precision interferometry, a heterodyne interferometer was constructed. A diagram of this interferometer is shown in figure 1.

A frequency stabilized Helium Neon (HeNe) laser operating at a wavelength of 632.8 nm was used as the coherent light source. The beam emitted from the output of the laser immediately encounters an acousto-optic modulator (AOM) and is split into different orders. The first order beam (which is shifted by 40 MHz due to the 40 MHz RF driving frequency of the AOM) is picked off with a mirror and sent into a polarizing beam splitter (PBS). The two orthogonal linear polarizations present within the light are split apart and sent in different directions. The \mathcal{S} -polarized light travels a distance from the PBS, to two stationary mirrors, and back to the PBS. This distance forms the reference arm of the interferometer. The \mathcal{P} -polarized light travels from the PBS, to a PZT mounted mirror, and back to the PBS. This distance is the signal arm of the interferometer and is controllable via a high-voltage amplifier attached to the PZT mirror.

The two polarizations are then recombined in the PBS and retro-reflected through the AOM to the laser. The beam then reflects off the front mirror of the laser and passes through the AOM once again, being shifted by an additional 40 MHz and having a total frequency shift of 80 MHz. Now, however, the beam exits the AOM superimposed over the zero order beam. The two orthogonal polarizations of the frequency shifted beam interfere with the respective orthogonal polarizations of the non-

shifted, zero order beam. This results in two orthogonally polarized 80 MHz, sinusoidal beat signals. These signals travel together until they reach a PBS where they are split apart. The \mathcal{S} -polarized beat signal travels up from the PBS and is incident upon a 125 MHz photodetector. The \mathcal{P} -polarized beat signal travels right from the PBS and is incident upon an additional 125 MHz photodetector. The signals coming from the two photodetectors are sinusoids each with a frequency of 80 MHz. Any movement of the PZT mirror results in a change in the path length of the signal arm of the interferometer and a change in the phase of the \mathcal{S} -polarized beat signal but not the \mathcal{P} -polarized beat signal. By measuring the change in phase between the two sinusoidal outputs of the photodetectors, one can keep track of very small changes in the PZT mirror's position. The change in the position of the mirror is related to the phase change by equation 3, where Δx is mirror movement and λ is the wavelength of the coherent light source.

$$\Delta x = \frac{\Delta \phi \lambda}{4\pi} \quad (3)$$

Phase changes are measured through the use of signal amplifiers, an analog quadrature detection system, and a LabVIEW interface. The signals from the photodetectors are passed through RF amplifiers and have their levels adjusted to match the input requirements of the quadrature phase detector which outputs the sine and cosine of the phase difference between the input signals. The LabVIEW interface serves to analyze these signals and retrieve the total relative phase change between the signals from either arm of the interferometer.

In order to test this system, the PZT mirror was driven with a 10 Hz triangle wave, and the output of the computer program was examined. Figures 2 and 3 show the beat signals before the quadrature detector and its sine and cosine output. Figure 4 shows part of the program's output, a clearly discernable 10 Hz triangle wave with a

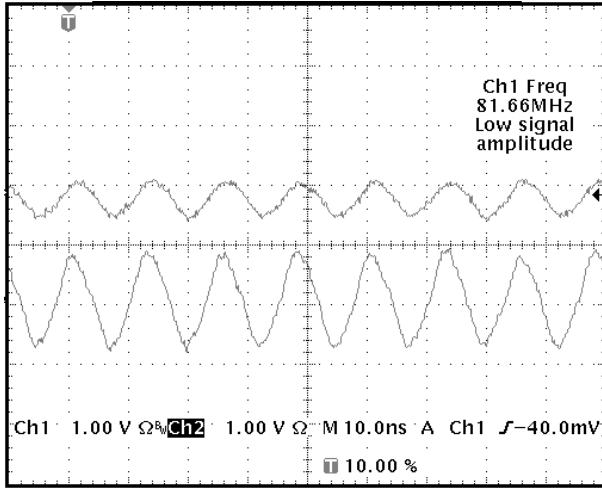


FIG. 2: The 80Mhz beat signals from the two photodetectors, one corresponding to each arm of the interferometer

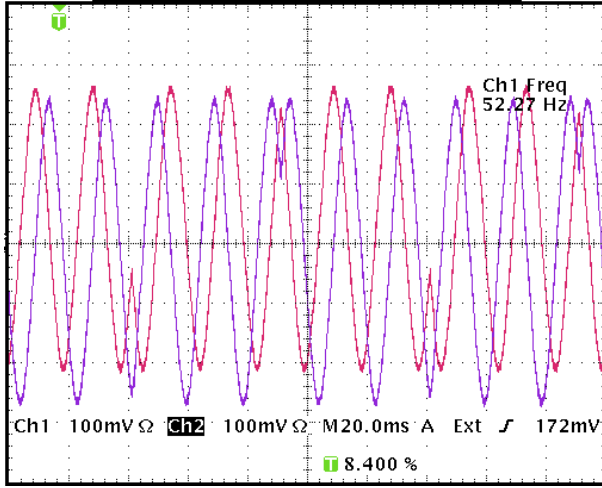


FIG. 3: $\sin(\Delta\phi)$ and $\cos(\Delta\phi)$ after the quadrature phase detector

peak to peak amplitude of 16.181 ± 0.002 radians, corresponding to 814.8 ± 0.1 nm mirror displacement.

In order to test the resolution limits of this system the PZT mirror was driven with a very small amplitude 10 Hz triangle wave. The smallest amplitude signal discernable was found to be 3.6 ± 0.1 nm peak to peak. The program's output for this case is shown in figure 5.

2. Quadrature phase detection scheme

To track the phase differences between the signals from the detectors, an analog quadrature detector (figure 6) was used in conjunction with a LabVIEW filtering and plotting interface. This interface has been developed by many other Bethel physics students over the years using National Instruments' LabVIEW.

The signal processing consisted of RF attenuators and

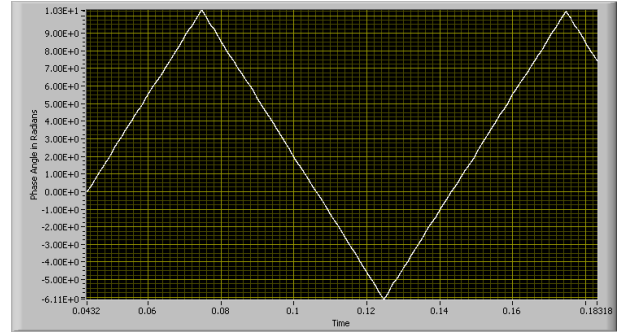


FIG. 4: Phase signal output from LabVIEW corresponding to 814.8 nm mirror travel in the PZT interferometer setup.

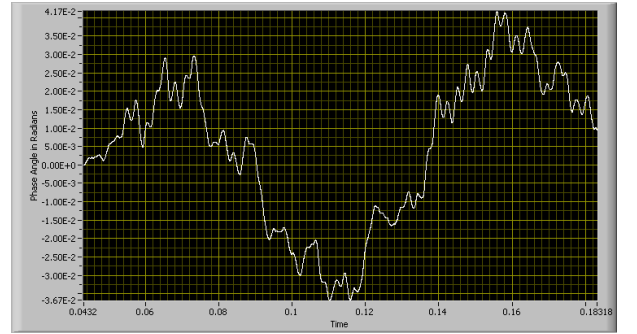


FIG. 5: Phase signal output from LabVIEW corresponding to 3.6 nm mirror travel in the PZT interferometer setup.

amplifiers to condition the signals for the input of the quadrature detector. The detector requires signals input at 9 dBm for the reference channel and 1 dBm for the signal channel. These correspond to $1.8 V_{pp}$ and $0.7 V_{pp}$ respectively for a sine wave at 40 Mhz. Through the analog electronics shown in figure 6 the sine and cosine of the phase difference between the signals from the two detectors can be obtained (figure 3). These signals were sent through low pass filters to attenuate the RF components of the signal. In most cases the signals were recorded with an oscilloscope then transmitted to LabVIEW via GPIB. Other input methods for LabVIEW are also available, but GPIB acquisition made it possible to take advantage of the powerful triggering and high temporal resolution of the Tektronics TEK3034b oscilloscope. The LabVIEW interface, at its core, takes the arctangent of the sine and cosine output from the quadrature system and tracks the total phase across the discontinuities at π and $-\pi$ of the arctangent function. Rolling averages as well as high and low pass filters in the LabVIEW program also made it possible to further attenuate noise and unwanted frequencies, isolating the desired features of the signal.

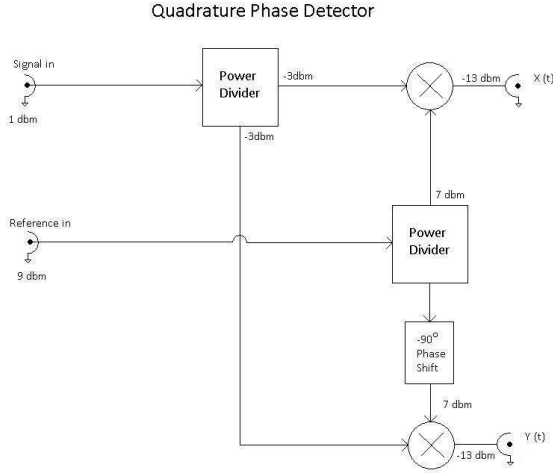


FIG. 6: Quadrature phase detector diagram showing reference and signal inputs and $\text{Sin}(\Delta\phi)$ $[x(t)]$ and $\text{Cos}(\Delta\phi)$ $[y(t)]$ outputs.

3. Heterodyne Mach-Zehnder Interferometer

The Mach-Zehnder Interferometer (figures 7 and 8) uses a polarizing beam splitter to separate the two orthogonal modes of the laser and send one through an AOM. The first order beam is shifted in frequency by 40 MHz after leaving the AOM. The two polarizations are then deflected by mirrors and recombined by another polarizing beam splitter. To obtain a 40 MHz difference in frequency between the two polarizations, an aperture is used to pass only the first order coming out of the AOM. After the beam is recombined, it then passes through a $\lambda/4$ wave plate which is aligned at 45 degrees to both orthogonal polarizations. This causes one of the two orthogonal bases defining the linear polarizations to be delayed by $\pi/2$, resulting in circular polarization. The two orthogonal linear polarizations are therefore transformed into left and right circular polarizations with a continually changing phase relationship difference due to the 40 MHz difference in their frequencies. The combination of these left and right circular polarizations results in a single linear polarization rotating at 20 MHz.

After the $\lambda/4$ wave plate, part of the beam is reflected off a non-polarizing beam splitter (a glass plate) and is sent to a detector. Before reaching the detector, the beam travels through a polarizer used to analyze the beam. Subsequently, a periodic waveform of 40 MHz is seen on an oscilloscope wired to the detector. This is caused when the rotating linear polarization aligns with the pass axis of the polarizer, resulting in maximum irradiance on the detector. After another ninety degrees of rotation, there is minimum irradiance on the detector. This cycle of maximum and minimum irradiance on the detector occurs two times per full cycle of rotation, yielding the 40 MHz waveform observed on the oscilloscope.

The rest of the beam is transmitted through the glass

plate and condensed by a converging lens. The beam then propagates through a TGG crystal placed inside of a solenoid. When a voltage is applied to this solenoid, a magnetic field is created which induces circular birefringence in the TGG crystal favoring one of the counter rotating circular polarizations and advancing the rotation or the resultant linear polarization. A picture of the five pass mirror, crystal and solenoid setup can be seen in figure 9.

The resultant beam experiences a net rotation of the linear polarization proportional to the magnetic field applied to the crystal. This rotation can be observed by sending the beam through a polarizer to another detector and comparing the two 40 MHz periodic waveforms, one picked off before the crystal and one after the crystal, displayed on an oscilloscope. The additional rotation angle of the linear polarization due to the Faraday Effect is measured by observing the relative phase difference between the two 40 MHz signals. The relationship between the rotation angle of the linear polarization and the phase difference between the two waveforms is shown below:

$$\Delta\theta = \frac{\Delta\phi}{2} \quad (4)$$

Again, LabVIEW was used to filter and obtain phase information from the sinusoidal signals after the quadrature phase detector. Thus measurements of the differential rotation of the linear polarization due to the Faraday Effect were acquired.

B. Measuring Verdet's Constant with a Polarimeter

To measure Verdet's constant, linearly polarized light was passed through a TGG crystal, centered inside a solenoid, 3 times, and the accumulated rotation of the beam was measured. This was accomplished by inserting a polarizing filter immediately after the laser allowing only one linear polarization to pass through the system. A three mirror system was then used to reflect the beam through the crystal twice, increasing the number of passes to three. Once the beam emerged from the mirrors and TGG crystal, an aperture was used to prevent all but the central part of the beam from entering the Glan-Thompson polarimeter. A power meter was placed after the polarimeter and used to find the angle of the polarimeter that minimized the irradiance. This angle was recorded and used as an initial angle from which to measure the angle of rotation caused by birefringence in the crystal. Figure 10 is a diagram of the optical setup used to find Verdet's constant.

Current was passed through the solenoid which created a magnetic field parallel to the direction of light propagation through the TGG crystal. This caused a net rotation in the linear polarization of the light which was then measured by rotating the polarimeter to minimize

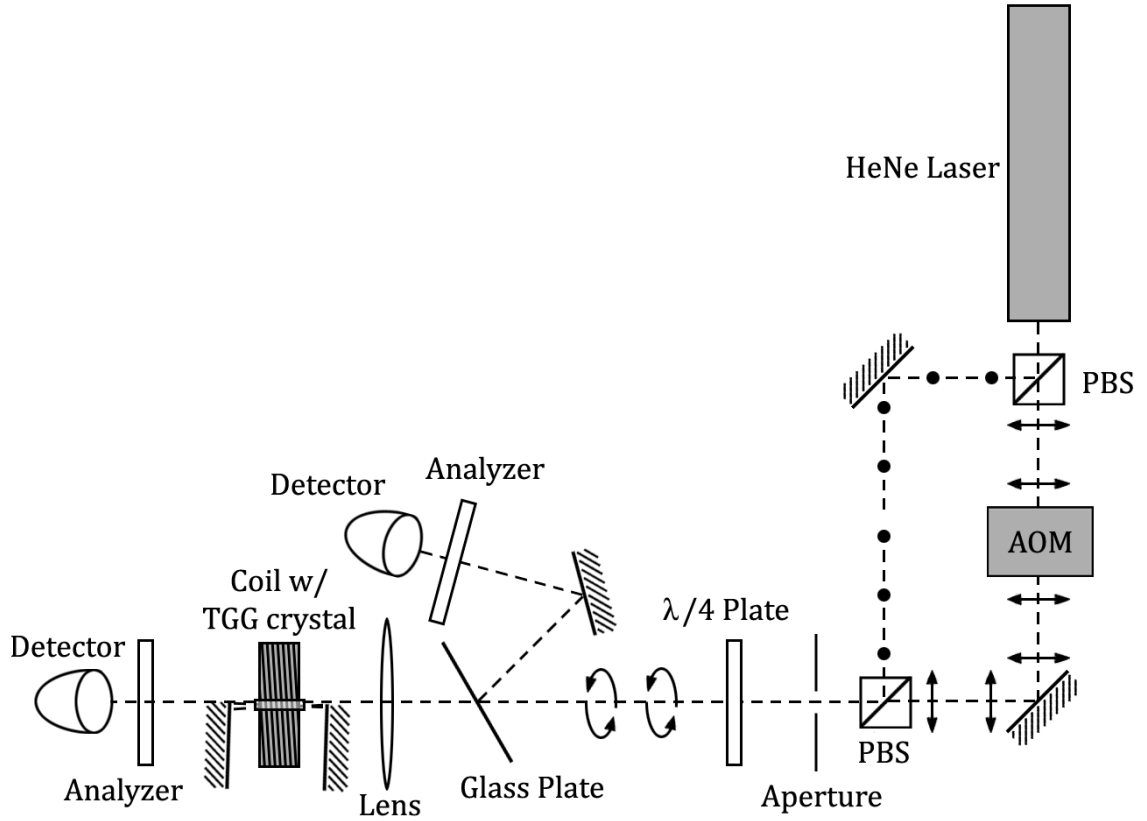


FIG. 7: Heterodyne Mach-Zehnder interferometer with TGG crystal. Magnetic fields parallel to the direction of propagation of light induce circular birefringence in the crystal, causing a net rotation in the linear polarization. This can be seen as a phase difference between the reference and signal beams.

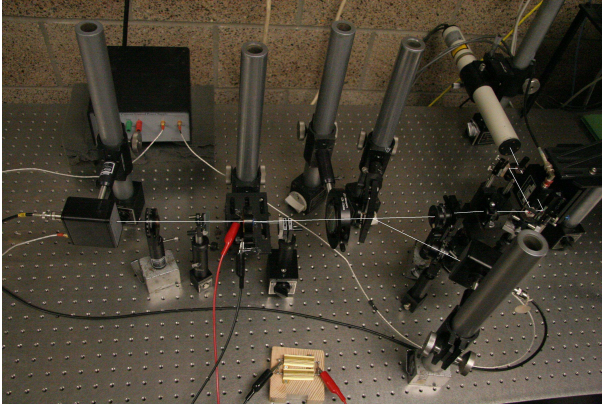


FIG. 8: The physical setup for our heterodyne interferometer with lines added to show the propagation of the light beams.

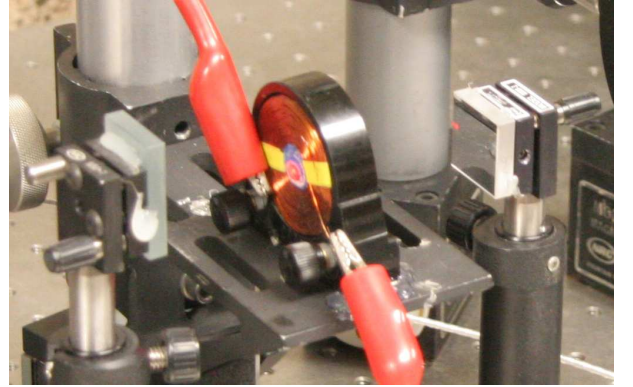


FIG. 9: Solenoid with TGG crystal at center. Mirrors are used to achieve five passes through the crystal causing a greater net rotation of the linear polarization.

the irradiance on the power meter. The current through the solenoid was recorded to calculate the magnitude of the magnetic field through the crystal and compare with the rotation angle. Current was provided through the use of a DC power supply capable of outputting currents greater than 4 amps at 16 volts. The solenoid used in this apparatus was measured to have an internal resis-

tance of $3.79 \pm 0.02 \, \Omega$ and an inductance of $4.40 \pm 0.01 \, \text{mH}$. Due to resistive heating of the solenoid, the current could not be calculated by measuring the voltage across the solenoid. To overcome this problem, a 100 Watt, $0.25 \, \Omega$ resistor was created by placing two 50 Watt, $0.50 \, \Omega$ resistors in parallel. This resistor was placed in series with the solenoid and the current could be calculated

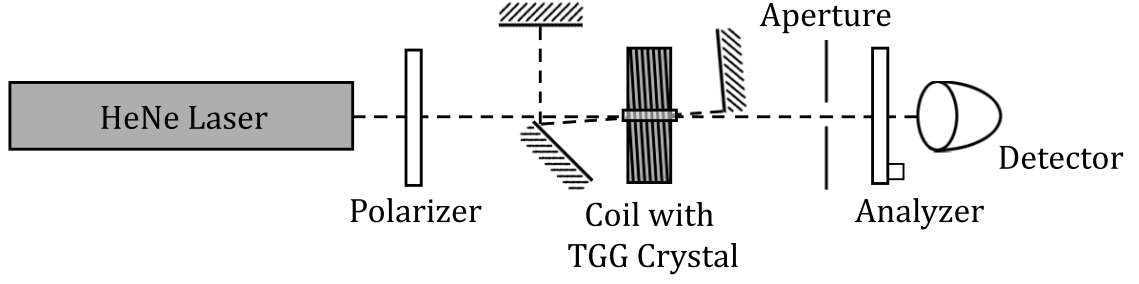


FIG. 10: Three pass system used to find Verdet's constant. The analyzer used was a Glan-Thompson Polarimeter with a measurement accuracy of ± 0.02 degrees.

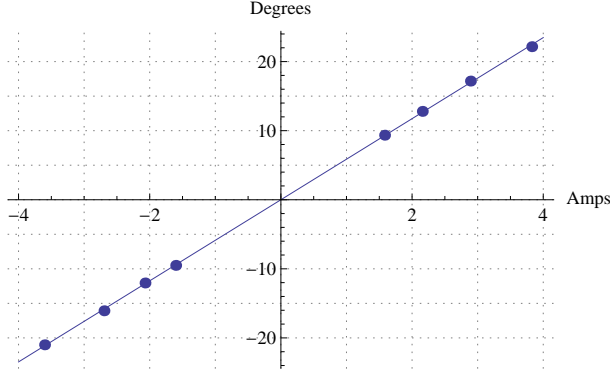


FIG. 11: The maximum magnetic field in the solenoid versus rotation of polarization. Line of best fit: $y = 5.8689x$

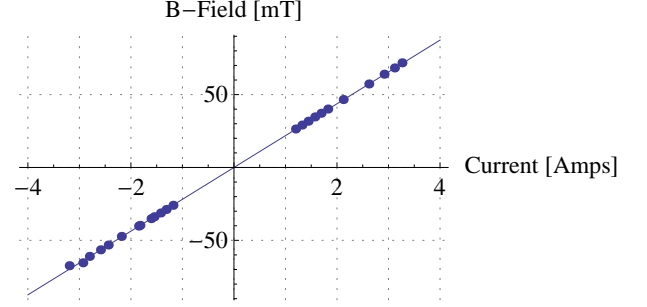


FIG. 12: The maximum magnetic field in the solenoid plotted against the applied current. Line of best fit: $y = 21.8484x$.

in real time by viewing the voltage across the resistor on an oscilloscope. The resistive heating of the $0.25 \, \Omega$ resistor was negligible for the currents used in this experiment and was not a significant source of error. Current was applied in both directions through the solenoid to account for both possible magnetic field directions that would cause a maximum Faraday effect in the TGG crystal. A linear relationship was found between the amount of current applied to the solenoid and the change in rotation angle (see figure 11).

The magnetic field at the center of the solenoid was measured using a F.W. Bell Tesla/Gauss meter, and the maximum field and corresponding current were recorded. Again, a linear relationship was found between the amount of current through the solenoid and magnitude of the magnetic field. The line of best fit intersecting the origin was calculated to obtain a general equation for finding the magnetic field at an arbitrary current. Figure 12 displays the maximum magnetic field versus current through the solenoid along with the least squares solution.

Using the data obtained by measuring the rotation angle, the maximum magnetic field was calculated for each corresponding current using the line of best fit. These points were then used to calculate the effective Verdet constant for a TGG crystal using equation(5) where N

$= 3$ and $L = 1.309 \pm 0.003 \, \text{cm}$. After averaging the results, the effective Verdet constant was found to be $0.412 \pm 0.005 \, \frac{\text{min}}{\text{gauss*cm}}$. This results in a 10.6% difference from the actual value of $0.461 \, \frac{\text{min}}{\text{gauss*cm}}$ obtained from a data sheet on TGG. This discrepancy is due to fringing effects on the ends of the solenoid which decreases the magnitude of the magnetic field at the ends of the crystal (see fig. 13) which in turn decreases the net rotation observed. The fringing can be taken into account by using equation 5 to describe the magnetic field along the length of the crystal where L is the width of the solenoid, a is radius of the central opening of the solenoid, and w is the radial thickness of the solenoid (see figure 13).

Equation 5 was used to calculate the average magnetic field along the length of the crystal. Using the corrected magnetic field, Verdet's constant was recalculated and found to be $0.449 \pm 0.005 \, \frac{\text{min}}{\text{gauss*cm}}$. A difference of 2.6% from the actual value was observed after correcting for fringing effects.

$$B(z) = \frac{\left(\frac{L}{2} - z\right) \ln \left[\frac{a+w+\sqrt{(a+w)^2 + (\frac{L}{2}-z)^2}}{a+\sqrt{a^2 + (\frac{L}{2}-z)^2}} \right] + \left(\frac{L}{2} + z\right) \ln \left[\frac{a+w+\sqrt{(a+w)^2 + (\frac{L}{2}+z)^2}}{a+\sqrt{a^2 + (\frac{L}{2}+z)^2}} \right]}{L \ln \left[\frac{a+w+\frac{1}{2}\sqrt{L^2+4(a+w)^2}}{a+\frac{1}{2}\sqrt{4a^2+L^2}} \right]} B_{max} \quad (5)$$

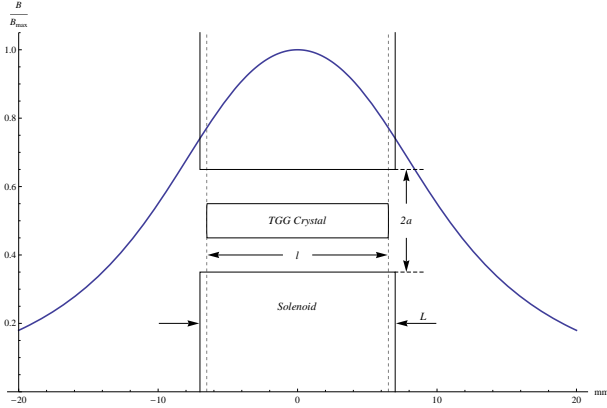


FIG. 13: Fringing effects in the magnetic field along the length of the crystal. Radial thickness of the solenoid: $w = 12.70$ mm, width of solenoid: $L = 14.02$ mm, radius of center opening: $a = 6.35$ mm, length of crystal: $l = 13.09$ mm.

III. RESULTS

A. Measurements with Interferometer

1. Time resolved magnetic field measurements

Measurements of Verdet's constant and time varying magnetic fields were made using the phase sensitive Mach-Zehnder interferometric polarimeter described above. Using the filtering capabilities of the LabVIEW interface, changes in phase between the signals from the two detectors in either system could be tracked to ± 0.002 radians over a few tenths of a second. The apparatus was constructed on a floating optics table to isolate it from low frequency vibrations in the building, and foam panels were used for acoustic shielding around the Mach-Zehnder portion of the apparatus. Care was taken to isolate the system from air currents; however, noise increased at acoustic frequencies, and some drift at < 0.5 Hz remained.

Several different sinusoidal voltages were applied to the solenoid, at 100 Hz, 5 kHz, and 50 Hz. For the 100 Hz signal, which was $200mV_{pp}$, the measured phase correlated well with the input. A $200 mV$ input, as measured across 0.25Ω corresponds to 0.8 Amps. Using the fit in figure 12, corrected for fringing, the magnetic field was calculated as follows:

$$0.800[Amps] * 201.035 \left[\frac{gauss}{Amp} \right] = 162[gauss] \quad (6)$$

A similar calculation using the measured phase difference shown in figure 19 and the data fit in figure 11, yields a field of 162 gauss, a difference of only 1.02%. The 5 kHz signal with measured phase shown in figure 20 exhibits a similar correlation between fields calculated from voltage and phase. These were 141 and 138 gauss respectively, a 2.17% difference.

For the 50 Hz signal, the system pushed the lower limits of the function generator and amplifier. The output of the amplifier had high frequency noise with an amplitude of about $10mV_{pp}$ which all but overwhelmed the input signal. Averaging the signal 128 times with an oscilloscope revealed a $3.2 \pm 0.5 mV_{pp}$ signal, which corresponds to a magnetic field of 2.6 ± 0.4 gauss. In addition, averaging the sine and cosine waveforms 128 times yielded a consistent change in phase of 0.00245 ± 0.0001 radians (figure 21), corresponding to a field of 2.42 ± 0.05 gauss.

Applying several other signals to the solenoid also revealed close correlation between the voltage and phase measurements. As the figures show, this was seen when stepping up the voltage with the power supply (figure 17) and when applying a quick current pulse to the coil by switching the power supply on and off (figure 14). As a check, the magnetic fields that should correspond to the voltage and phase for each input above were calculated with the corrected data fits from the polarimeter measurements and plotted against each other (figures 15 and 18). However, in a puzzling turn they did not match as expected. The calculations were checked and re-checked, but the results remained. This was puzzling because the polarimeter results were so consistently linear and the phase measurements so precise.

2. Calculations of Verdet's Constant

As we calculated Verdet's constant for the sets of data, the cause of the differing Verdet's constants became apparent. Figure 16 gives Verdet's constant calculated point by point for the pulse shown in figure 14. The results were self-consistent, but Verdet's constant varied. This observation was confirmed when Verdet's constant was calculated for the sinusoidal data sets using the peak to peak values for magnetic field and phase change. The results are shown in table I.

Since the sine waves were low current, 0.8 amps or less compared to upwards of 4 amps for some the pulses and stepped measurements, they didn't require the solenoid to dissipate much power which kept the TGG crystal near room temperature. This is important because TGG

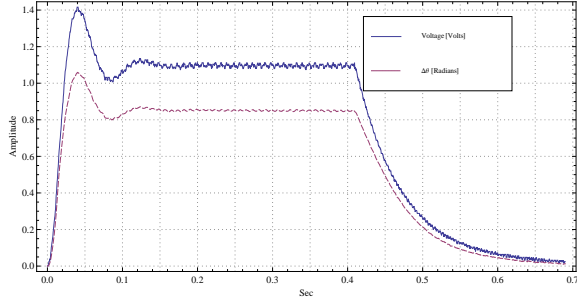


FIG. 14: Voltage across 0.25Ω and phase measurements made while quickly switching on and off the power supply attached to the solenoid around the TGG crystal. Note the ringing due to the coil's impedance.

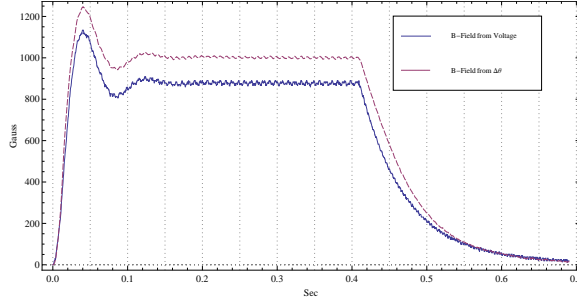


FIG. 15: The average magnetic field through the crystal as calculated from the phase and voltage measurements

shows a strong inverse relationship with temperature, about 12 minutes of angle per degree celsius for 5 passes through a 1.309 cm TGG crystal [2]. In the interferometric polarimeter discussed above, a thermocouple inserted alongside the crystal revealed more than 10 degrees celsius change in temperature over a few minutes after 3 amps was applied for around 30 seconds. This would correspond to an attenuation of 2 degrees of rotation over 5 passes, enough to change a calculated Verdet's constant by several hundredths. The Glan-Thompson polarimeter measurements were made quickly, with the current ap-

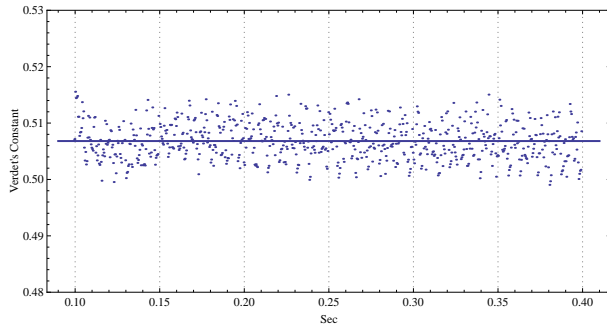


FIG. 16: The average Verdet's constant and the constant as calculated point by point in the flat region of a pulse, after the ringing and before the power supply was turned off.

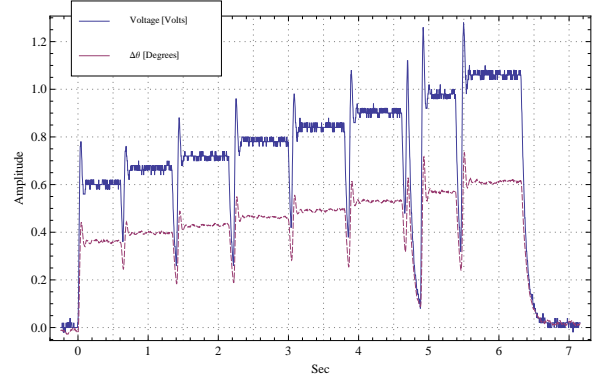


FIG. 17: Voltage across 0.25Ω and phase measurements made while stepping the voltage up with the power supply.

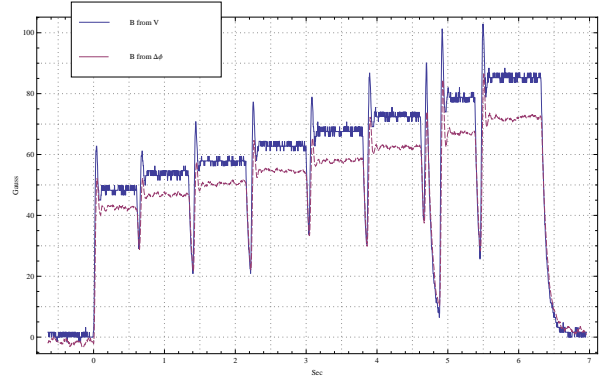


FIG. 18: The average magnetic field through the crystal as calculated from the phase and voltage measurements while stepping the voltage up with the power supply

plied for only a few seconds at a time with long pauses between measurements so they showed strong correlation with the sinusoidal measurements. The temperature in the lab varied greatly from day to day and, for the stepped and pulsed measurements, less care was taken to apply the current for short periods of time. This data was often being taken after several other high current measurements.

Method	V_c	Difference
Polarimeter	0.449 ± 5	2.6%
Pulse 1	0.442 ± 7	4.1%
Pulse 2	0.509 ± 7	10.4%
Pulse 3	0.390 ± 7	15.4%
Stepped	0.391 ± 7	15.1%
Sine 5 Hz	0.453 ± 3	1.7%
Sine 100 Hz	0.438 ± 3	5.0%
Sine 5 kHz	0.443 ± 3	3.9%
Accepted Value	0.461	

TABLE I: Values for Verdet's constant in $[\frac{\text{min}}{\text{gauss*cm}}]$ that were obtained with our various measurement methods

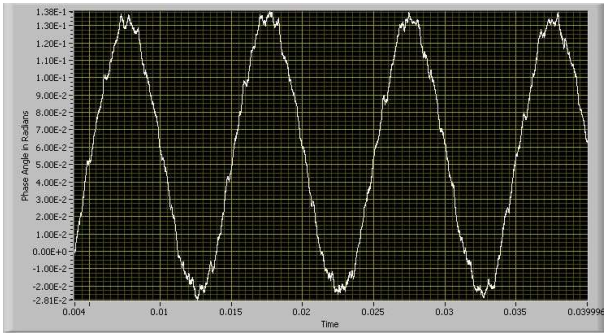


FIG. 19: Input voltage signal: 100 Hz, 200 mV_{pp} , sine wave. B-field calculated from input = 160 gauss. B-field from measured phase = 162 gauss. Difference = 1.02%

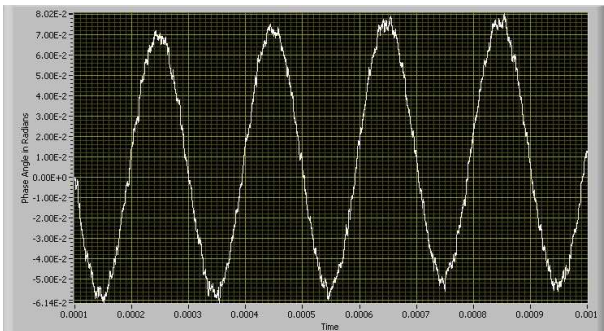


FIG. 20: Input voltage signal: 5000 Hz Sine Wave 176 mV_{pp} . B-field calculated from input = 141 gauss. B-field from measured phase = 138 gauss. Difference = 2.17%

IV. CONCLUSION

Precise interferometry, coupled with the Faraday Effect in a TGG crystal, proved to be an effective method

for measuring magnetic fields of various amplitudes and frequencies. The current apparatus is capable of accurately measuring magnetic fields of high frequencies limited to the acoustic range by the cutoff filters present in the electronic mixing system. Periodic magnetic

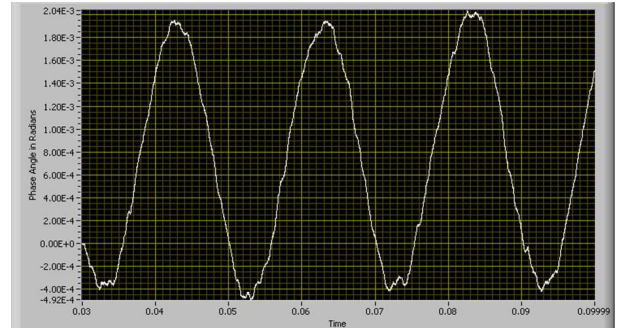


FIG. 21: Input voltage signal: 50 Hz Sine Wave using Scopes Average Function 3.2 mV_{pp} . B-field from voltage = 2.6 ± 0.4 gauss. B-field from phase = 2.42 ± 0.05 gauss.

phenomena with amplitudes as small as 2.42 ± 0.05 gauss were also measured. Finally, a corrected Verdet's constant for TGG was measured to be $0.449 \pm 0.005 \frac{\text{min}}{\text{gauss*cm}}$, a 2.6% difference from the accepted value of $0.461 \frac{\text{min}}{\text{gauss*cm}}$.

A. Acknowledgments

We would like to thank Dr. Peterson for his constant guidance and wise insight into this project. Also, many thanks to Dr. Hoyt for a great semester!

-
- [1] Hecht, Eugene. and Zajac, Alfred. Optics Eugene Hecht, with contributions by Alfred Zajac Addison-Wesley Pub. Co., Reading, Mass. : 1987
 - [2] Norman P. Barnes and Larry B. Petway, "Variation of the Verdet constant with temperature of terbium gallium

- garnet," J. Opt. Soc. Am. B 9, 1912-1915 (1992)
- [3] R. W. Peterson et. al, "Faraday Effect Time Resolved Magnetic Field Measurements."